Laser-printed emissive metasurface implemented with a planar thin-film resonator

Myeongkyu Lee*, *Yeongseon* Kim, *Dongkyun* Kang, and *Jaeyong* Kim

Materials Science and Engineering Department, Yonsei University, Seoul 03722, Korea

Abstract. Optical security is a promising application of metasurfaces because light has large degrees of freedom in metasurfaces. Although many different structures/materials have been proposed for this purpose, the fabrication of dynamic metasurfaces in a straightforward and scalable manner while maintaining a high security level remains a significant challenge. Herein, a metasurface consisting of a phase-changing $Ge_2Sb_2Te_5$ (GST) layer and a thin metal back reflector is presented to space-selectively and dynamically control the infrared emission of the surface by a spatially modulated pulsed laser beam. Unlike conventional laser processes using a focused beam, the employed laser printing is an expanded beam-based parallel process that enables the fabrication of wafer-sized emission patterns. Owing to the multispectral responses of GST, mutually independent visible and infrared images can be printed in one region. Grayscale emission patterns can also be obtained by gradually modulating the spatial profile of the laser beam, which makes the replication of laser-printed emission patterns extremely difficult. These encouraging features are experimentally verified using rigid and flexible substrates, indicating that the presented emissive metasurface has the potential for use as an effective platform for anti-counterfeiting.

1 Introduction

A metasurface is an artificial interface with subwavelength thickness that manipulates light by spatially arranged structures called meta-atoms. With the advent of spatial control over the phase and amplitude of electromagnetic waves, metasurfaces have enabled the realization of optical cloaking, super-resolution imaging, and planar optics, which cannot be achieved with the existing bulky optical elements. One of the promising applications of metasurfaces is in the field of optical security [1–5]. The demand for anti-counterfeiting methods with high security levels has continuously increased, particularly in the era of pandemics. The large degrees of freedom (i.e., phase, amplitude, and polarization) in metasurfaces make them suitable for use in optical security technologies against forgery.

Traditional anti-counterfeiting schemes (intaglio, guilloche, and latent image) allow non-experts to easily detect forgeries, but these material-based techniques can be easily replicated. As metasurface-based methods can provide significantly higher security levels, a number of different structures and materials have been investigated, including meta-holograms, polarization-selective metasurfaces, viewing angle-dependent metasurfaces, and Malus metasurfaces. However, in these approaches, as the security level increases, decoding the encoded information becomes more complex and can be performed only by experts with a specific setup. Additionally, the fabrication of metasurfaces operating in the visible range requires a nanofabrication process such as electron-beam lithography, which limits their scalability.

In this study, we present a parallel laser-printing process to independently control the IR and visible responses of a GST metasurface. This enabled the printing of different visible and IR images in one region. Both images can be easily captured using visible and IR cameras by non-experts, providing a simple forgery-detecting scheme. However, the replication of the thermal image becomes extremely difficult as its emission profile is gradually modulated by an expanded laser beam through a grayscale photomask. The printing process is scalable and can produce wafer-sized patterns. Lithography requires photoresist (PR) steps (PR deposition, development, and etching), whereas the fabrication of this GST metasurface involves only thin-film deposition and laser irradiation. All of these provide favorable features for anti-counterfeiting.

2 Results and discussion

The metasurface had a planar cavity structure comprising a GST film on top of a metal back reflector, which was stationed on a substrate. Our approach was to print crystallization patterns inside and on the surface of an amorphous GST film using a spatially modulated pulsed laser beam. The visible reflection of the cavity was determined solely by the top-surface structure of the GST film because of the short penetration depth of visible light into GST, whereas the IR emission depended on the internal structure of the film.

* Corresponding author: myeong@yonsei.ac.kr

Fig. 1 shows the structure of a GST cavity formed on a Si substrate, along with its visible and IR images. Here, *a*-GST represents amorphous GST and *c*-GST refers to crystalline GST. To fabricate the cavity, a 100-nm Cr layer and a 200-nm *a*-GST film were sequentially deposited onto an Al-coated Si substrate using a shadow mask (QR shadow mask). The surface of the *a*-GST film was irradiated by a laser beam passing through the shadow mask. Subsequently, an additional 200-nm *a*-GST film was uniformly coated over the structure. Finally, the surface of the coated GST film was irradiated by a laser beam that was spatially modulated through a photomask (barcode image).

The difference in reflectance between *c*-GST and *a*-GST phases leads to a visual contrast. The visible reflectance of a GST cavity depends solely on the surface structure (i.e., phase) of the GST film owing to the short penetration depth of visible light into GST. Therefore, the visible image of the cavity is independent of its internal structure and is determined by the surface crystallization pattern. In other words, the visible image is defined by the photomask pattern used in the final step. In contrast, the thermal image of a cavity is strongly influenced by its internal structure. The areas with a 400-nm-thick GST film on top of the Cr layer exhibit much stronger emission than those with the 200-nm-thick GST film without Cr. The former has a GST thickness of 400 nm, resulting in an emissivity peak in the detection range (7.5–13 μm) of ordinary IR cameras. The embedded Cr and *c*-GST layers also increase the emissivity; Cr is more absorptive than Al in the IR range, and *c*-GST is also more absorptive than *a*-GST in the same range. The latter has a smaller GST thickness of 200 nm, resulting in an emissivity peak outside the detection range of the IR camera.

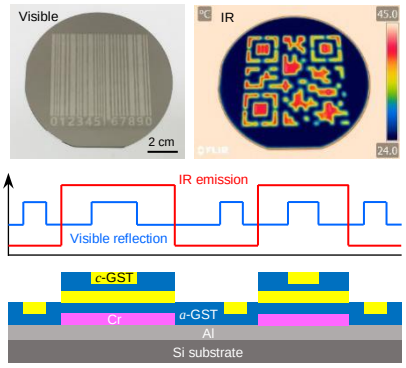

Fig. 1. Structure of a GST cavity fabricated on a Si substrate along with its visible and IR images. *a*-GST represents amorphous GST and *c*-GST refers to crystalline GST.

Another GST emitter was fabricated on a Korean banknote of 1000 won using the same QR shadow mask and a different photomask containing an "Einstein image" (**Fig. 2**); 1000 won is worth approximately one dollar. Unlike the Si substrate, the banknote substrate has a rough surface; nevertheless, the visible image recorded was clearly recognizable. The emitter was also highly flexible; no material delamination or image distortion was observed the substrate was completely folded.

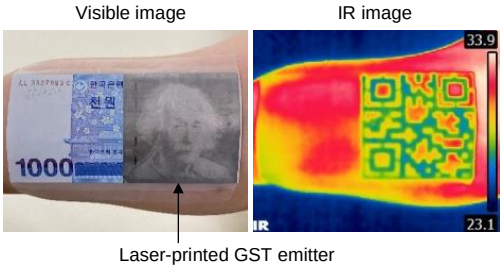

Fig. 2. Visible and IR images of a GST emitter fabricated on a Korean banknote.

3 Conclusion

In this study, emissivity-modulated GST emitters were fabricated on rigid and flexible substrates. The emissivity was spatially controlled by forming crystalline GST phases within the amorphous GST film using a spatially modulated pulsed laser beam and by selectively depositing a Cr layer on the Al back reflector. The multispectral properties of GST enabled different visible and IR images to be simultaneously recorded in the same area. The fact that a single emitter can exhibit different visible and IR images is particularly attractive for optical security applications, including anti-counterfeiting.

This work was supported by National Research Foundation of Korea(NRF) grants funded by the Korean government(MSIT) (2020R1A2C2003575 and 2022M3H4A1A02046445) and a Korea Agency for Infrastructure Technology Advancement(KAIA) grant funded by the Ministry of Land, Infrastructure and Transport (Grant 21CTAP-C163910-01).

References

1. I. Kim, J. Jang, G. Kim, J. Lee, T. Badloe, J. Mun, J. Rho, Nat. Commun. **12**, 3614 (2021)
2. Z. Li, C. Chen, Z. Guan, J. Tao, S. Chang, Q. Dai, Y. Xiao, Y. Cui, Y. Wang, S. Yu, G. Zheng, S. Zhang, Laser Photonics Rev. **14**, 2000032 (2020)
3. J. Deng, L. Deng, Z. Guan, J. Tao, G. Li, Z. Li, Z. Li, S. Yu, G. Zheng, Nano Lett. **20**, 1830 (2020)
4. C. Zhang, F. Dong, Y. Intaravanne, X. Zang, L. Xu, Z. Song, G. Zheng, W. Wang, W. Chu, X. Chen, Phys. Rev. Appl. **12**, 034028 (2019)
5. F. Yue, C. Zhang, X. Zang, D. Wen, B. Gerardot, S. Zhang, X. Chen, Light: Sci. Appl. **7**, 17129 (2018)